Analysis of Nucleotide Insertion and Extension at 8-Oxo-7,8-dihydroguanine by Replicative T7 Polymerase exo$^-$ and Human Immunodeficiency Virus-1 Reverse Transcriptase Using Steady-State and Pre-Steady-State Kinetics†

Laura Lowe Furge‡ and F. Peter Guengerich*

Department of Biochemistry and Center in Molecular Toxicology, Vanderbilt University School of Medicine, Nashville, Tennessee 37232-0146

Received October 31, 1996; Revised Manuscript Received March 27, 1997⊗

ABSTRACT: Pre-steady-state kinetics of incorporation of dCTP and dATP opposite site-specific 8-oxo-7,8-dihydroguanine (8-oxoGua), in contrast to dCTP insertion opposite G, were examined as well as extension beyond the lesion using the replicative enzymes bacteriophage polymerase T7 exo$^-$ (T7$^-$) and HIV-1 reverse transcriptase (RT). These results were compared to previous findings for *Escherichia coli* repair polymerases I (KF$^-$) and II (pol II$^-$) exo$^-$ [Lowe, L. G., & Guengerich, F. P. (1996) *Biochemistry 35*, 9840−9849]. HIV-1 RT showed a very high preference for insertion of dATP opposite 8-oxoGua, followed by pol II$^-$, T7$^-$, and KF$^-$. Steady-state assays showed k_{cat} consistently lower than pre-steady-state polymerization rates (k_p) for insertion of dCTP opposite G or 8-oxoGua and insertion of dATP opposite 8-oxoGua. Pre-steady-state kinetic curves for the addition of dCTP opposite 8-oxoGua or G by KF$^-$, pol II$^-$, and T7$^-$ were all biphasic, with a rapid initial single-turnover burst followed by a slower multiple turnover rate, while addition of dATP opposite 8-oxoGua by these polymerases did not display burst kinetics. With HIV-1 RT, addition of dATP opposite 8-oxoGua displayed burst kinetics while addition of dCTP did not. Analyses of the chemical step by substitution of phosphorothioate analogs for normal dNTPs suggest that the chemistry is rate-limiting during addition of dCTP and dATP opposite 8-oxoGua by KF$^-$, pol II$^-$, and T7$^-$; HIV-1 RT did not show a chemical rate-limiting step during addition of dATP opposite 8-oxoGua. Kinetic assays performed with various dCTP concentrations indicate that dCTP has a higher K_d and lower k_p for incorporation opposite 8-oxoGua compared to G with all four enzymes. The $K_{d,app}^{dATP}$ values for KF$^-$, pol II$^-$, and T7$^-$ incorporation of dATP opposite 8-oxoGua, estimated in competition assays, were found to be 3−10-fold greater than the K_d^{dCTP}. Likewise, the $K_{d,app}^{dCTP}$ for HIV-1 RT incorporation of dCTP opposite 8-oxoGua was found to be 10-fold greater than the K_d^{dATP}. The repair enzymes (KF$^-$ and pol II$^-$) efficiently extended the 8-oxoGua·A pair; extension of 8-oxoGua·C was severely impaired, whereas the replicative enzymes (T7$^-$ and HIV-1 RT) extended both pairs, with faster rates for the extension of the 8-oxoGua·A pair. On the basis of these findings, the fidelity of all four enzymes during replication of 8-oxoGua depends on contributions from the apparent K_d, the ease of base pair extension, and either the rate of conformational change before chemistry or the rate of bond formation.

Exposure of cells to exogenous and endogenous sources of reactive chemicals and oxygen species leads to the formation of DNA adducts (Miller & Miller, 1966, 1971). DNA adducts, via their miscoding potential when replicated by DNA polymerases, are precursors to mutagenic events which, if unrepaired, can contribute to carcinogenesis (Basu & Essigmann, 1988, 1990; Feig & Loeb, 1994). The miscoding potential of DNA adducts results from the ability of DNA adducts to form incorrect base pairs, which may escape editing by DNA polymerases and repair by DNA repair systems (Echols & Goodman, 1991; Marnett & Burcham, 1993). Thus, polymerase fidelity during replication of DNA adducts is a contributor to the prevention of mutation and cancer.

The most abundant DNA adduct formed from reactive oxygen species is 8-oxoGua,[1] which is found at levels of 10−250 molecules per 10^6 guanines in some mammalian tissues and at higher frequencies in some disease states (Ames et al., 1993; Marnett & Burcham, 1993; Malins et al., 1995; Shimoda et al., 1994). 8-OxoGua causes G to T transversions when replicated by all DNA polymerases examined to date and is thought contribute to cumulative cancer risk (Shigenaga et al., 1994; Marnett & Burcham, 1993). The noted miscoding potential of 8-oxoGua has been suggested to be due to the structural similarity of an 8-oxoGua·A base pair to a T·A base pair (Lipscomb et al.,

† This work was supported in part by United States Public Health Service (USPHS) Grants R35 CA44353 and P30 ES00267. L.L.F. was supported in part by USPHS Training Grant T32 ES07028.

* Author to whom correspondence should be addressed. Telephone: (615) 322-2261. Fax: (615) 322-3141. E-mail: guengerich@toxicology.mc.vanderbilt.edu.

‡ Formerly Laura G. Lowe.

⊗ Abstract published in *Advance ACS Abstracts,* May 15, 1997.

[1] Abbreviations: 8-oxoGua, 8-oxo-7,8-dihydroguanine; dNTPαS, α-thiodeoxynucleoside triphosphate; EDTA, (ethylenedinitrilo)tetraacetic acid; Gua, guanine; T7, bacteriophage T7 DNA polymerase exo$^+$; T7$^-$, bacteriophage T7 DNA polymerase exo$^-$; HIV-1, human immunodeficiency virus-1; HIV-1 RT, HIV-1 reverse transcriptase; KF$^+$, *Escherichia coli* polymerase I (Klenow fragment) exo$^+$; KF$^-$, *E. coli* polymerase I (Klenow fragment) exo$^-$; pol II$^-$, *E. coli* polymerase II exo$^-$; Tris, tris(hydroxymethyl)aminomethane; DTT, dithiothreitol; BSA, bovine serum albumin; AMV RT, avian myeloblastosis virus reverse transcriptase.

S0006-2960(96)02726-2 CCC: $14.00

Scheme 1: General Kinetic Mechanism for DNA Polymerases (Johnson, 1993)[a]

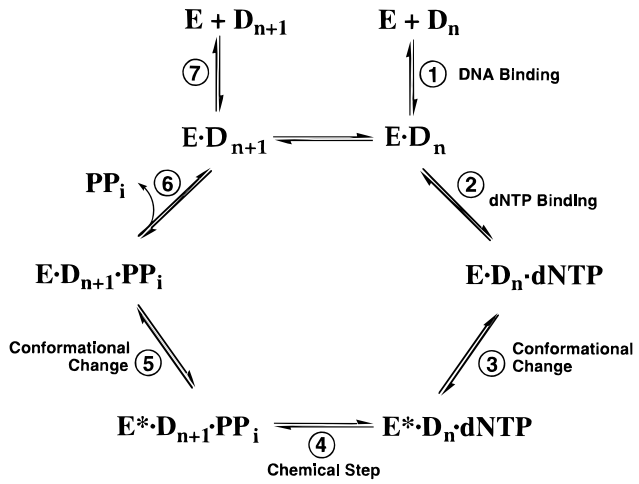

[a] Individual steps are numbered and identified. Assays described in this study allow only for a single round of nucleotide addition followed by substrate release (step 7). Abbreviations: E = polymerase, D_n = DNA, E* = conformational change in polymerase, and D_{n+1} = DNA extended by one base.

1995; McAuley-Hecht et al., 1994; Kouchakdjian et al., 1991).

Cells are equipped with a variety of DNA polymerases with varying responsibilities in maintaining the stability and integrity of the genome, in terms of replicating different types of DNA substrates. The fidelity of individual polymerases, then, contributes to the overall fidelity of DNA replication and the prevention of mutagenesis and carcinogenesis. Two families of DNA polymerases that fulfill the requirements for maintenance of genome integrity have been identified: replicative and repair enzymes. Both families of enzymes catalyze the rapid and selective incorporation of dNTPs and in many cases use exonuclease proofreading to increase their fidelity. Some polymerases that are structurally related and conform to similar reaction pathways (Scheme 1) have been found to behave differently in terms of kinetics during replication of DNA adducts (Cai et al., 1993; Lowe & Guengerich, 1996; Reha-Krantz et al., 1996; Frey et al., 1995). Our studies (Lowe & Guengerich, 1996) of the pre-steady-state replication of 8-oxoGua by the *Escherichia coli* repair enzymes KF$^-$ and pol II$^-$ showed that the rates of nucleotide binding, phosphodiester bond formation, and base pair extension differed for insertion of dCTP and dATP opposite 8-oxoGua.

The present study compares the pre-steady-state replication of an oligonucleotide containing a carcinogen-modified base (8-oxoGua) by the replicative enzymes T7$^-$ from T7 bacteriophage and HIV-1 RT (as compared to the repair enzymes KF$^-$ and pol II$^-$ from *E. coli*) (Lowe & Guengerich, 1996). The replicative enzymes discussed in the present study, T7$^-$ and HIV-1 RT, were selected as model replicative enzymes due to their well-established mechanisms, their availability in large quantities for pre-steady-state assays, and their lack of complicating accessory proteins as opposed to the case of *E. coli* polymerase III with its more than 20 accessory polypeptides (Perler et al., 1996; Johnson, 1993). T7$^-$ (80 kDa) is functionally and structurally homologous to KF$^-$ (Johnson, 1993). In addition, T7$^-$ forms a heterodimer with *E. coli* thioredoxin to obtain high processivity and fidelity (Kornberg & Baker, 1992). HIV-1 RT forms a heterodimer of p66 and p51 subunits (the latter of which is a cleavage product of p66) and has the lowest fidelity of all polymerases and RTs studied to date (Kornberg & Baker, 1992). The catalytic mechanisms for stepwise polymerization by T7$^-$ and HIV-1 RT have been well characterized (Patel et al., 1991; Donlin et al., 1991; Wong et al., 1991; Kati et al., 1992) (Scheme 1). In the present study, kinetic differences between the *E. coli* repair and the viral replicative enzymes were found as well as distinctions between KF$^-$, pol II$^-$, and T7$^-$ and the low-fidelity enzyme HIV-1 RT.

EXPERIMENTAL PROCEDURES

Enzymes. The overproducer strains for T7$^-$ (Ap179 pGP1/pGP5X-) and thioredoxin (SK398 pBHK8) were provided by K. A. Johnson (Pennsylvania State University, University Park, PA). T7$^-$ and thioredoxin were purified to electrophoretic homogeneity (Laemmli, 1970) as described by Patel et al. (1991) and Lunn et al. (1984), respectively. Protein concentrations were estimated using an ϵ_{280} of 144 mM^{-1} cm^{-1} for T7$^-$ and an ϵ_{280} of 13.7 mM^{-1} cm^{-1} for thioredoxin. Purified T7$^-$ was stored in small aliquots at −70 °C in 20 mM potassium phosphate buffer (pH 7.4) containing 0.1 mM EDTA, 1.0 mM DTT, and 50% glycerol (v/v) for over 1 year prior to use without apparent loss of activity. Thioredoxin was also stored in small aliquots at −70 °C in 50 mM Tris-HCl buffer (pH 8.5) containing 3 mM EDTA and 50% glycerol (v/v). T7$^-$ was reconstituted immediately prior to use as described (Patel et al., 1991). Briefly, fresh DTT (0.5 M) was added to a solution of thioredoxin to a final DTT concentration of 5 mM. Reduced thioredoxin and T7$^-$ were then combined in 40 mM Tris-HCl buffer (pH 7.5) containing 1.0 mM EDTA, 1.0 mM DTT, 0.1 mg of BSA/mL, and 50 mM NaCl so that the molar ratio of T7$^-$ to thioredoxin was 1:20. The activity of T7$^-$ was determined to be nearly 100% in active-site titration experiments (*vide infra*).

S. Hughes (Frederick Cancer Facility, Frederick, MD) provided the HIV-1 RT (His) protein-overproducing system for the HIV-1 RT. The HIV-1 RT (His) protein construct is similar to that described by LeGrice and Grüninger-Leitch (1990), in which the plasmid simultaneously expresses the HIV-1 p66 RT subunit and the HIV-1 protease. The overexpressed p66 can then be processed to p51 by the protease to generate nearly equimolar amounts of each subunit. The p66/p51 heterodimers accumulate in the bacteria and are purified simultaneously by metal chelate chromatography as described (Le Grice & Grüninger-Leitch, 1990) with minor modification (provided by P. Boyer, Frederick Cancer Facility). The protein concentration was determined using an ϵ_{280} of 261 mM^{-1} cm^{-1} for the heterodimer (Kati et al., 1992). Purified HIV-1 RT was stored in small aliquots at −70 °C in 50 mM Tris-HCl buffer (pH 8.0) containing 2 mM EDTA, 1.0 mM DTT, and 50% glycerol (v/v) for 1 year prior to use. Active-site titration experiments (*vide infra*) were used to determine the activity of RT to be ∼45%. Concentrations reported in this paper are based upon the A_{280} values with corrected active concentrations indicated as well.

Nucleoside Triphosphates. Unlabeled ultrapure grade dNTPs were purchased from Pharmacia Biotech (Uppsala, Sweden); (S_p)-dNTPαSs were purchased from United States Biochemical Corp. (Cleveland, OH), and all radioisotopes were purchased from DuPont-New England Nuclear (Boston, MA).

Oligonucleotides. The sequences chosen for primer (24-mer) and template (36-mer) were adapted from a combination

of a 12/16-mer duplex used previously in this lab (Lowe & Guengerich, 1996) and the sequences used by Johnson and his associates for T7 (Patel et al., 1991; Wong, 1991; Donlin et al., 1991). The 24-mer and 8-oxoGua-modified 36-mer oligonucleotides were purchased as "trityl-on" oligonucleotides from Midland Certified Reagent Co. (Midland, TX). The 8-oxoGua phosphoramidite provided to Midland for preparation of 8-oxoGua-modified 36-mer was purchased from Glen Research (Sterling, VA). All other oligonucleotides were synthesized as trityl-on oligonucleotides on an Expedite Nucleic Acid Synthesis System (Millipore Corp., Bedford, MA). Oligonucleotides were detritylated and purified by NENSORB PREP cartridges (E. I. du Pont de Nemours & Co., Inc., Boston, MA), followed by purification by gel electrophoresis as described (Lowe & Guengerich, 1996). The purity of all oligonucleotides was determined to be >99% as evaluated by capillary gel electrophoresis on a Beckman P/ACE 2000 instrument (Beckman, Fullerton, CA) using an "ssDNA 100" gel capillary and "TRIS-borate-urea buffer" from the manufacturer (see the Supporting Information). Samples were applied at −5 kV and run at −10 kV (30 °C). Concentrations of purified oligonucleotides were estimated by UV absorbance (260 nm) from spectra determined using a modified Cary-14/OLIS spectrophotometer (On-Line Instrument Systems, Bogart, GA). Extinction coefficients were as follows: 24-mer, $\epsilon_{260} = 224$ mM^{-1} cm^{-1}; 36-mer, $\epsilon_{260} = 312$ mM^{-1} cm^{-1}; 25-mer with 3′-A, $\epsilon_{260} = 237$ mM^{-1} cm^{-1}; and 25-mer with 3′-C, $\epsilon_{260} = 230$ mM^{-1} cm^{-1} (Borer, 1975).

Primer End Labeling and Primer/Template Annealing. Primers were 5′-end-labeled by T4 polynucleotide kinase (Gibco BRL Life Technologies, Grand Island, NY) with [γ-^{32}P]ATP (3000 Ci/mmol) as previously described (Boosalis et al., 1987) and as modified in this laboratory (Lowe & Guengerich, 1996).

Steady-State Incorporation of dCTP or dATP Opposite Gua or 8-OxoGua. The general approach of Boosalis et al. (1987) was used, as modified in this laboratory (Lowe & Guengerich, 1996) and here. Steady-state reaction mixtures with T7⁻ and unmodified 24/36-mer (control template) contained 1.2 nM T7⁻ and 100 nM primer/template duplex (final concentrations). T7⁻ steady-state reactions with the 8-oxoGua-modified 24/36-mer contained 5.1 nM T7⁻ and 100 nM duplex DNA. Reaction mixtures with HIV-1 RT and the control template contained 9.4 nM HIV-1 RT and 100 nM duplex unmodified DNA. Reaction mixtures with HIV-1 RT and 8-oxoGua-modified 24/36-mer contained 100 nM (final concentration) duplex DNA and 24 nM (final concentration) HIV-1 RT for addition of dCTP and 12.2 nM (final concentration) RT for addition of dATP opposite 8-oxoGua. Reactions were initiated by the addition of an equal volume of dNTP (various concentrations) in 100 mM Tris-HCl buffer (pH 7.4) containing 25 mM $MgCl_2$ (buffer A) (final concentrations of Tris-HCl and $MgCl_2$ were 50 and 12.5 mM, respectively) to preincubated enzyme/DNA solution. All reactions were quenched with twice the reaction volume of 20 mM EDTA at pH 7.4 (13 mM final concentration). Reaction times for T7⁻ with control template plus dCTP or dATP and for 8-oxoGua-modified template plus dCTP or dATP were 3 and 5 min, respectively. Reaction times for HIV-1 RT with control template plus dCTP or dATP, for 8-oxoGua-modified template plus dCTP, and for 8-oxoGua-modified template plus dATP were 4, 5, and 3.5 min, respectively. Control experiments were performed to ensure that the reactions remained in the linear range. Reaction mixtures with T7⁻ included 40 mM Tris-HCl (pH 7.5) buffer containing 1.0 mM EDTA, 50 mM NaCl, 1.0 mM DTT, and 0.1 mg of BSA/mL. Reaction mixtures with HIV-1 RT contained 50 mM Tris-HCl (pH 7.5) and 50 mM NaCl. All steady-state reactions were done in an 8.0 μL reaction volume and were done in triplicate. Products were analyzed by electrophoresis on a denaturing gel [16% acrylamide (w/v), 1.5% bisacrylamide (w/v), and 8.0 M urea]. A Molecular Dynamics Model 400E Phosphorimager (Molecular Dynamics Inc., Sunnyvale, CA) equipped with ImageQuant software version 3.3 was used to measure incorporation of radioactivity, and the results were analyzed using a k·cat computer program (Biometallics, Princeton, NJ) as described (Lowe & Guengerich, 1996).

Pre-Steady-State Experiments. Pre-steady-state (rapid quench) experiments were carried out in a KinTek Quench-Flow Apparatus (model RQF-3, KinTek Corp., State College, PA). Reactions were started by rapid mixing of primer/template/polymerase mixtures (21.5 μL) with either dCTP or dATP in buffer A (26.3 μL) and then quenched with an equal volume of 0.6 M EDTA at pH 7.4. Products were analyzed by gel electrophoresis and quantitated as described above. Pre-steady-state experiments, except where indicated, were fit to the burst equation $y = A(1 - e^{-k_p t}) + k_{ss}t$, where A = burst amplitude, k_p = pre-steady-state rate of nucleotide incorporation, t = time, and k_{ss} = steady-state rate of nucleotide incorporation.

Competition Assays. Competition assays with dCTP and dATP were done to approximate $K_{d,app}$ values for T7⁻ binding of dATP and for HIV-1 RT binding of dCTP in reactions with 8-oxoGua-containing template. The assays were done using the general approach described above for the rapid quench experiments, except that the dNTP solution contained both dCTP and dATP at various concentrations as well as a 125 μCi spike of [α-^{32}P]dCTP in reactions with T7⁻ or [α-^{32}P]dATP in reactions with HIV-1 RT and the 24/36-mer was not labeled. Reactions with T7⁻ were done with the following (final concentration) combinations of dCTP and dATP: 20 μM dCTP/0 μM dATP, 20 μM dCTP/20 μM dATP, 20 μM dCTP/60 μM dATP, 20 μM dCTP/200 μM dATP, 60 μM dCTP/0 μM dATP, 60 μM dCTP/20 μM dATP, 60 μM dCTP/60 μM dATP, and 60 μM dCTP/200 μM dATP. Reactions with HIV-1 RT were done with the following final concentration combinations of dATP and dCTP: 20 μM dATP/0 μM dCTP, 20 μM dATP/20 μM dCTP, 20 μM dATP/60 μM dCTP, and 20 μM dATP/200 μM dCTP. Products were analyzed by electrophoresis as described earlier. Bands corresponding to insertion of labeled dNTP were quantitated and compared to the concentration of product formed under similar circumstances with no competing dNTP and with labeled primer and cold dNTP. In the competition assays, as the concentration of competing cold dNTP was increased, incorporation of the radiolabeled dNTP was decreased.

Measurement of Extension Past C·8-OxoGua, A·8-OxoGua, C·Gua, and A·Gua Pairs. Rapid quench experiments were done to determine the efficiency of extension past an 8-oxoGua base pair with a 25-mer primer containing either an A or a C in the 3′-position opposite 8-oxoGua. All reactions were initiated by rapid mixing of primer/template/enzyme solution with 220 μM dGTP (final concentration) in buffer A. Products were analyzed as described above.

Table 1: Oligonucleotides[a]

control 24/36-mer	5′- GCCTCGA**GCCGCAGACGCAG**
	3′- CGGAGCT**CGGCGTCTGCGTCGCTC**CTGCGGCT
8-oxoGua-modified 24/36-mer	5′- GCCTCGA**GCCGCAGACGCAG**
	3′- CGGAGCT**CGGCGTCTGCGTCGCTC**CTGCGGCT
8-oxoGua-modified 25A/36-mer	5′- GCCTCGA**GCCGCAGACGCAGA**
	3′- CGGAGCT**CGGCGTCTGCGTCGCTC**CTGCGGCT
8-oxoGua-modified 25C/36-mer	5′- GCCTCGA**GCCGCAGACGCAGC**
	3′- CGGAGCT**CGGCGTCTGCGTCGCTC**CTGCGGCT

[a] G denotes position of 8-oxoGua.

Kinetic Simulations. In order to estimate a set of rate constants consistent with the mechanism in Scheme 1, kinetic simulations modeling the observed kinetic curves for dNTP incorporation were done by mathematical analysis using HopKINSIM version 1.7, obtained from C. Freiden (Washington University, St. Louis, MO) (Barshop et al., 1983), on a Macintosh Power PC 7100 computer (Apple Computer Inc., Cupertino, CA) equipped with SoftwareFPU version 3.03 (John Neil & Associates, Cupertino, CA).

RESULTS

DNA Substrate Selection. Steady-state assays were first attempted with the 12/16-mer sequence used in previous studies with KF$^-$ and pol II$^-$ (Lowe & Guengerich, 1996). The sequence corresponding to the 12/16-mer is shown in boldface in Table 1. The steady-state parameters obtained from assays with T7$^-$ were not what were expected on the basis of literature reports for normal incorporation reactions (Johnson, 1993) and from previous work in this lab with KF$^-$ and pol II$^-$ (Lowe & Guengerich, 1996) (i.e., K_m and k_{cat} for insertion of dCTP opposite Gua were 16 μM and 0.034 s^{-1}, respectively, and the K_m and k_{cat} for insertion of dCTP or dATP opposite 8-oxoGua were ~200 μM and ~0.004 s^{-1}, respectively). Also, extension by HIV-1 RT was very slow, even with a high concentration of enzyme. Furthermore, when initial pre-steady-state experiments were performed with T7$^-$, the resulting time progress curves did not show the characteristic biphasic response for a normal incorporation reaction by T7$^-$ and the active-site titration yielded a high K_d^{DNA} (for insertion of dCTP opposite Gua). Because the enzymes had been stored at −70 °C for several months prior to use, we considered the possibility that they had lost activity. The other possibility was that the choice of DNA substrate was inappropriate for these enzymes. Some precedent for the later explanation is found in the work of Patel et al. (1991) with T7$^-$ and of Patel et al. (1995) with HIV-1 RT. Patel et al. (1991) reported that the smaller substrates that had been used with KF showed weaker binding affinity for T7. Patel et al. (1995) reported that DNA substrates with a short overhang showed weaker binding affinity for HIV-1 RT, although the efficiency of nucleotide insertion was not altered. On the basis of these findings, a DNA substrate with a larger duplex region and longer overhang was prepared using the 12/16-mer from previous work (boldface in Table 1) as the central portion of the new substrate and adding duplex and overhang sequence from the substrate used by Johnson and his associates with T7 (Patel et al., 1991; Donlin et al., 1991; Wong et al., 1991). The 24/36-mer substrate was prepared and purified as described (Experimental Procedures). The possibility that a loss of enzyme activity was the cause of the low k_{cat} and high K_m values was then eliminated when active-site titration experiments were performed with the 24/36-mer DNA substrate (*vide infra*). Briefly, T7$^-$ displayed nearly 100% activity, and HIV-1 RT showed ~45% activity, which is similar to the activity of HIV-1 RT reported by Kati et al. (1992) and Spence et al. (1995).

Table 2: Steady-State Kinetic Parameters for T7$^-$ and HIV-1 RT

	T7$^-$		HIV-1 RT	
	K_m (μM)	k_{cat} (s^{-1})	K_m (μM)	k_{cat} (s^{-1})
G·C[a]	2.5 ± 0.6	0.12 ± 0.01	0.3 ± 0.1	0.010 ± 0.001
8-oxoG·C[a]	55 ± 7	0.019 ± 0.001	61 ± 17	0.002 ± 0.001
8-oxoG·A[a]	138 ± 45	0.027 ± 0.004	34 ± 5	0.015 ± 0.001
f[b]	0.6		14	

[a] The base in the oligomer is presented first (G or 8-oxoGua), followed by the dNTP used. [b] The apparent misinsertion frequency for dNTP incorporation opposite 8-oxoGua is defined as $f = (k_{cat}/K_m)_{dATP}/(k_{cat}/K_m)_{dCTP}$ (Boosalis *et al.*, 1987, 1989), with substitution of k_{cat} for V_{max} in this work.

Steady-State Kinetics of dCTP and dATP Incorporation Opposite 8-OxoGua and dCTP Incorporation Opposite Gua. Steady-state assays with T7$^-$ and unmodified or 8-oxoGua-modified 24/36-mer used ~83- and ~20-fold excesses of duplex DNA over enzyme, respectively (Table 2). The difference in k_{cat} for insertion of dCTP opposite Gua and insertion of dCTP or dATP opposite 8-oxoGua was ~5-fold (0.12 ± 0.01 versus 0.019 ± 0.001 and 0.027 ± 0.004 s^{-1}). The K_m values for insertion of dCTP and dATP opposite 8-oxoGua were ~20- and ~55-fold greater, respectively, than the K_m for insertion of dCTP opposite Gua (55 ± 7 and 138 ± 45 versus 2.5 ± 0.6 μM). Under the conditions of these assays, there was no apparent incorporation of dATP opposite Gua, for comparison to dCTP incorporation (i.e., the rate was too low to measure). The misinsertion frequency (f) of T7$^-$ for dNTP incorporation opposite 8-oxoGua was estimated to be 0.6 using the relationship $f = (k_{cat}/K_m)_{dATP}/(k_{cat}/K_m)_{dCTP}$ (Boosalis et al., 1987, 1989). This analysis predicts an ~37% misinsertion of dATP opposite 8-oxoGua by T7$^-$.

Steady-state assays for incorporation of dCTP opposite Gua by HIV-1 RT were accomplished with an ~11-fold excess of DNA over enzyme. Under the conditions of these assays and up to a dATP concentration of 1.6 mM (final), there was no observable insertion of dATP opposite Gua by HIV-1 RT (for comparison to insertion of dCTP opposite Gua). In HIV-1 RT reactions with 8-oxoGua-containing 24/36-mer and dCTP and dATP, DNA was in an ~4- and ~8-fold excess enzyme, respectively (Table 2). Insertion of dATP opposite 8-oxoGua yielded a k_{cat} similar to that for the normal incorporation reaction of dCTP opposite Gua (0.015 ± 0.001 and 0.010 ± 0.001 s^{-1}, respectively), while K_m values were ~100-fold different (34 ± 5 μM for dATP versus 0.3 ± 0.1 μM for dCTP). Insertion of dCTP opposite 8-oxoGua proceeded with a k_{cat} ~5-fold lower (0.002 ± 0.001 s^{-1}) and a K_m ~200-fold greater (61 ± 17 μM) than those for insertion of dCTP opposite Gua. Also, the K_m and k_{cat} parameters for insertion of dCTP opposite 8-oxoGua were ~2-fold higher and ~7-fold lower, respectively, than the values for insertion of dATP opposite 8-oxoGua. The fidelity of HIV-1 RT for insertion opposite 8-oxoGua, estimated as described above, was 14, predicting 93% misincorporation of dATP opposite 8-oxoGua.

Pre-Steady-State Kinetics of dCTP and dATP Incorporation Opposite 8-OxoGua and dCTP Incorporation Opposite

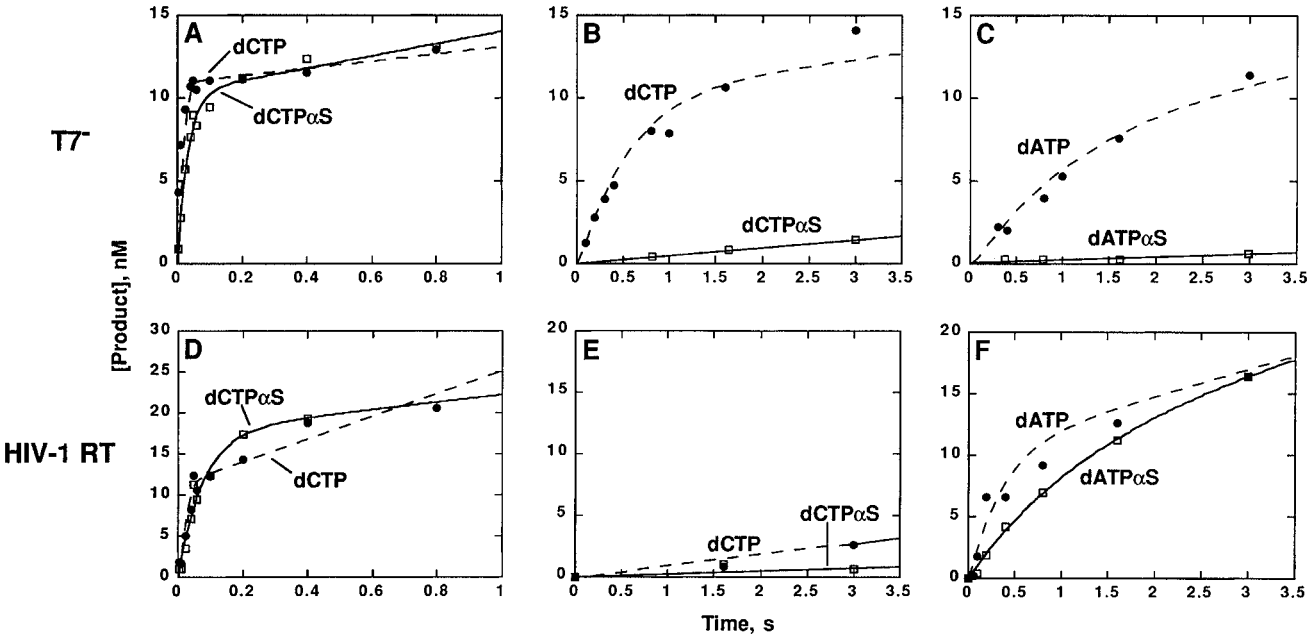

FIGURE 1: Pre-steady-state kinetics of nucleotide incorporation. (A) T7⁻ (12 nM, preincubated with 102 nM unmodified 24/36-mer) was mixed with a solution of dCTP (220 μM) in buffer A in the rapid quench instrument (●). For analysis of the elemental effect on phosphodiester bond formation, T7⁻ (12 nM, preincubated with 102 nM unmodified 24/36-mer) was mixed with a solution of dCTPαS (220 μM) in buffer A in the rapid quench instrument (□). All reactions were quenched by the addition of EDTA to 0.3 M. The data obtained for normal dNTP incorporation were fit by computer simulation (KINSIM) using Scheme 1 and the rate constants in Table 3 and are indicated with a dashed line. The data for phosphorothioate analog incorporation were fit to the burst equation $y = A(1 - e^{-k_p t}) + k_{ss}t$, where A = burst amplitude, k_p = pre-steady-state rate of nucleotide incorporation, t = time, and k_{ss} = steady-state rate of nucleotide incorporation, and are indicated with a solid line. (B) T7⁻ (12 nM, preincubated with 102 nM 8-oxoGua-modified 24/36-mer) was mixed with a solution of dCTP (220 μM) in buffer A (●) or with a mixture of dCTPαS (220 μM) in buffer A (□) as described above. (C) T7⁻ (12 nM, preincubated with 102 nM 8-oxoGua-modified 24/36-mer) was mixed with a solution of dATP (220 μM) in buffer A (●) or with a solution of dATPαS (220 μM) in buffer A (□) as described above. (D) HIV-1 RT [27 nM (12 nM active concentration), preincubated with 102 nM unmodified 24/36-mer] was mixed with a solution of dCTP (220 μM) (●) or dCTPαS (220 μM) in buffer A (□) as described above. (E) HIV-1 RT [27 nM (12 nM active concentration), preincubated with 102 nM 8-oxoGua-modified 24/36-mer] was mixed with a solution of dCTP (220 μM) (●) or dCTPαS (220 μM) (□) in buffer A as described above. (F) HIV-1 RT [27 nM (12 nM active concentration), preincubated with 102 nM 8-oxoGua-modified 24/36-mer] was mixed with a solution of dATP (220 μM) (●) or dATPαS (220 μM) (□) in buffer A as described above.

Table 3: Pre-Steady-State Rate Constants[a]

		T7⁻			HIV-1 RT		
	k	G·C	8-oxoG·C	8-oxoG·A	G·C	8-oxoG·C	8-oxoG·A
E + D ⇌ ED	+1	≥10^8	≥10^8	≥10^8	≥10^8	≥10^8	≥10^8
	−1	1.5	0.9	0.9	1.2	3.7	3.7
ED+N ⇌ EDN	+2	(≥10^8)	(≥10^8)	(≥10^8)	(≥10^8)	(≥10^8)	(≥10^8)
	−2	1−2.5 × 10^3	10^5	0.5−1.0 × 10^5	10^3	10^5	10^5
EDN ⇌ XDN	+3	50−100	7.0	1.0	100	0.1	10
	−3	[0.06]	[0.06]	[0.06]	[0.06]	[0.06]	[0.06]
XDN ⇌ XFP	+4	1000	50	10−25	1000	10	>100
	−4	[0.003]	[0.003]	[0.003]	[0.003]	[0.003]	[0.003]
XFP ⇌ EFP	+5	(>100)	(>100)	(>100)	(>100)	(>100)	(>100)
	−5	[1.4 × 10^{-4}]	[1.4 × 10^{-4}]	[1.4 × 10^{-4}]	[1.4 × 10^{-4}]	[1.4 × 10^{-4}]	[1.4 × 10^{-4}]
EFP ⇌ EF+P	+6	[10^4]	[10^4]	[10^4]	[10^4]	[10^4]	[10^4]
	−6	(≥10^8)	(≥10^8)	(≥10^8)	(≥10^8)	(≥10^8)	(≥10^8)
EF ⇌ E + F	+7	0.1−0.6	0.07	0.01	0.1−0.6	0.01	0.01−0.5
	−7	[≥1.2 × 10^7]	[≥1.2 × 10^7]	[≥1.2 × 10^7]	[≥1.2 × 10^7]	[≥1.2 × 10^7]	[≥1.2 × 10^7]

[a] Data were modeled using the kinetic simulation program HopKINSIM as described in Experimental Procedures. Values shown in the table were derived starting with our experimental values, assumed values (in parentheses), and literature precedents (in brackets; Eger & Benkovic, 1992; Tan et al., 1994; Patel et al., 1991). Abbreviations are as in Scheme 1 with the following substitutions: X = E*, F = D_{n+1}, and P = PP_i. All values are expressed in units of s^{-1} or M^{-1} s^{-1}, depending upon the reaction order. See the text for discussion.

Gua. Pre-steady-state experiments were done with 2−10-fold excesses of DNA over enzyme. Reactions were initiated by the rapid mixing of enzyme preincubated for ~5 min at room temperature with 24/36-mer and a saturating solution of dNTP (220 μM, final)/$MgCl_2$ and then quenched by the addition of EDTA (pH 7.4) to 0.3 M over a time range varying from 5 ms to 10 s. The pre-steady-state burst curves for incorporation of dCTP opposite Gua and 8-oxoGua by T7⁻ are shown in panels A and B of Figure 1, respectively. The pre-steady-state progress curve for incorporation of dATP opposite 8-oxoGua is shown in Figure 1C. The dotted lines for dNTP incorporation represent a fit of the data to the kinetic mechanism shown in Scheme 1 and the rate constants shown in Table 3. The single-turnover reaction for incorporation of dCTP opposite Gua is over in ~60 ms, while the single-turnover phase is longer for insertion of dCTP opposite 8-oxoGua, ending at ~800 ms. For insertion of dATP opposite 8-oxoGua, there is no large differentiation

between single and multiple turnovers.

The pre-steady-state burst curve for insertion of dCTP opposite Gua by HIV-1 RT is shown in Figure 1D. The dotted lines represent a fit of the data to the kinetic mechanism shown in Scheme 1 and the rate constants shown in Table 3. The single-turnover reaction in this case is over at ~200 ms. Incorporation of dCTP opposite 8-oxoGua by HIV-1 RT, shown in Figure 1E, is a very slow reaction, while incorporation of dATP opposite 8-oxoGua occurs quite readily with a biphasic response (Figure 1F). This is the first observation of a biphasic response in the misincorporation of dATP opposite 8-oxoGua. The burst amplitude for incorporation of dATP opposite 8-oxoGua is, however, less than expected on the basis of the active enzyme concentration and the dCTP/Gua reactions. It appears that not all complexes of HIV-1 RT, 8-oxoGua-containing duplex DNA, and dATP are in competent conformations that allow dATP incorporation.

Phosphorothioate Elemental Analysis. Previous studies have shown that chemistry is at least a partially rate-limiting step for addition of dNTPs opposite 8-oxoGua by KF$^-$ and pol II$^-$ (Lowe & Guengerich, 1996). This possibility was addressed in these experiments by the substitution of phosphorothioate analogs for the normal dNTPs. The substitution of dCTPαS for dCTP had little effect on the rate of product formation by T7$^-$ and unmodified 24/36-mer (Figure 1A). However, as in the case of KF$^-$ and pol II$^-$, substitution of dCTPαS and dATPαS for dCTP and dATP, respectively, yielded reduced rates of product formation with T7$^-$ when the substrate was 8-oxoGua-containing DNA (Figure 1B,C). The solid lines for dNTPαS incorporation represent a fit of the data to the burst equation described in Experimental Procedures. The elemental effects were ~1.2, ~13, and ~10 for incorporation of dCTPαS opposite Gua and 8-oxoGua and dATPαS opposite 8-oxoGua, respectively.

Substitution of dCTPαS for dCTP had no measurable effect on the burst rate of product formation with HIV-1 RT and unmodified DNA substrate (Figure 1D). However, elemental analysis studies of incorporation of dCTPαS and dATPαS opposite 8-oxoGua by HIV-1 RT yielded results different from those found with KF$^-$, pol II$^-$, and T7$^-$; i.e., neither substitution generated a significant elemental effect, although reactions with HIV-1 RT, 8-oxoGua, and dCTP are not active enough for a definitive interpretation (Figure 1E,F). This is the first time the rate of incorporation of dCTP or dATP opposite 8-oxoGua has *not* been shown to be at least partially limited by chemistry in such "mismatch" experiments. The solid lines for dNTPαS incorporation represent a fit of the data to the burst equation described in Experimental Procedures. Elemental effects of ~1.1, ~4, and ~2 were measured with HIV-1 RT for incorporation of dCTPαS opposite Gua, dCTPαS opposite 8-oxoGua, and dATPαS opposite 8-oxoGua, respectively.

Active-Site Titrations and Determination of K_d^{DNA}. Changes in burst amplitude were measured as the concentration of DNA substrate was varied to determine the enzyme active-site number and the K_d for binding DNA substrate (Figure 2). T7$^-$ was preincubated with increasing concentrations (2−130 nM) of 24-mer annealed to either unmodified or 8-oxoGua-modified 36-mer (Figure 2A). The enzyme/DNA solution was then mixed with 220 μM dCTP in buffer A, and product formation was measured in the usual way. Product formation increased with increasing DNA concentration independent of the presence of Gua or 8-oxoGua in the template (Figure 2A). Also, the burst amplitude corresponded to the UV-determined concentration of T7$^-$ protein in the reaction mixtures, indicating that all of the enzyme population was involved in the catalytic process. The K_d values for T7$^-$ binding the unmodified and 8-oxoGua-containing DNA substrates were estimated to be 15 ± 8 and 9 ± 4 nM, respectively, by plotting the burst amplitudes from Figure 2A,B against the concentration of DNA and then fitting the data to the quadratic equation $[E{\cdot}D] = 0.5(K_d + E_t + D_t) - [0.25(K_d + E_t + D_t)^2 - E_tD_t]^{1/2}$, where E_t = [total enzyme], D_t = [total DNA], and K_d = dissociation constant for the reaction E + D ⇌ E·D (Figure 3A).

In the determination of HIV-1 RT K_d values for binding unmodified and 8-oxoGua-modified DNA substrates, the same approach described above for T7$^-$ was used with the change being that 220 μM dATP was used in reactions with 8-oxoGua-containing 24/36-mer, since HIV-1 RT shows no burst of product formation for incorporation of dCTP opposite 8-oxoGua but does for incorporation of dATP opposite 8-oxoGua. The burst amplitude for incorporation of dCTP opposite Gua was ~45% of the UV-determined concentration of HIV-1 RT (Figure 2C), indicating that ~45% of the enzyme was catalytically competent. Burst amplitudes for incorporation of dCTP opposite Gua and of dATP opposite 8-oxoGua obtained by analysis of the data in Figure 2C,D using the burst equation were plotted against [DNA] and the data fit to the quadratic equation $[E{\cdot}D] = 0.5(K_d + E_t + D_t) - [0.25(K_d + E_t + D_t)^2 - E_tD_t]^{1/2}$ to determine K_d. The K_d for HIV-1 RT binding of unmodified 24/36-mer was 12 ± 5 nM, while the K_d for binding 8-oxoGua-containing 24/36-mer was 37 ± 11 nM (Figure 3B). There is a difference between these dissociation constants, which reflects a further reduction of burst amplitude seen in experiments with dATP, 8-oxoGua-containing DNA, and HIV-1 RT as compared to the burst heights at similar concentrations of HIV-1 RT during incorporation of dCTP opposite Gua by HIV-1 RT. This result suggests that there may be pools of competent and incompetent conformers of HIV-1 RT during extension with dATP of the 8-oxoGua-containing 24/36-mer.

Determination of the Pre-Steady-State Parameters K_d and k_p for dNTP Incorporation. The concentration of dNTP was varied, and the dNTP dependence of product formation was monitored in progress curves (Figure 4 and data not shown). These curves were also used for kinetic simulations to estimate the rate constants in Table 3 which govern Scheme 1. The pre-steady-state rates were determined by single-exponential analysis by plotting $\ln(P_n - P_t)$ versus t to yield lines of slope $-k_{obs}$, where P_n is the concentration of product at the end of the burst phase, P_t is the concentration of product at time t in the burst phase, and k_{obs} is the observed rate of the burst reaction (results not shown). The rates were then plotted against the change in [dNTP] and fitted to the hyperbola $k_{obs} = [k_p[\text{dNTP}]/([\text{dNTP}] + K_d)]$, which describes the reaction equation

$$E{\cdot}D + N \overset{K_d}{\rightleftharpoons} E{\cdot}D{\cdot}N \overset{k_p}{\rightleftharpoons} E{\cdot}D_{n+1}{\cdot}PP_i$$

where E = enzyme, D = 24/36-mer oligomer, N = dNTP, D_{n+1} = 25/36-mer product oligomer, and PP_i = pyrophosphate. In this scheme, k_p is an experimentally determined parameter that contains contributions from the rates of both

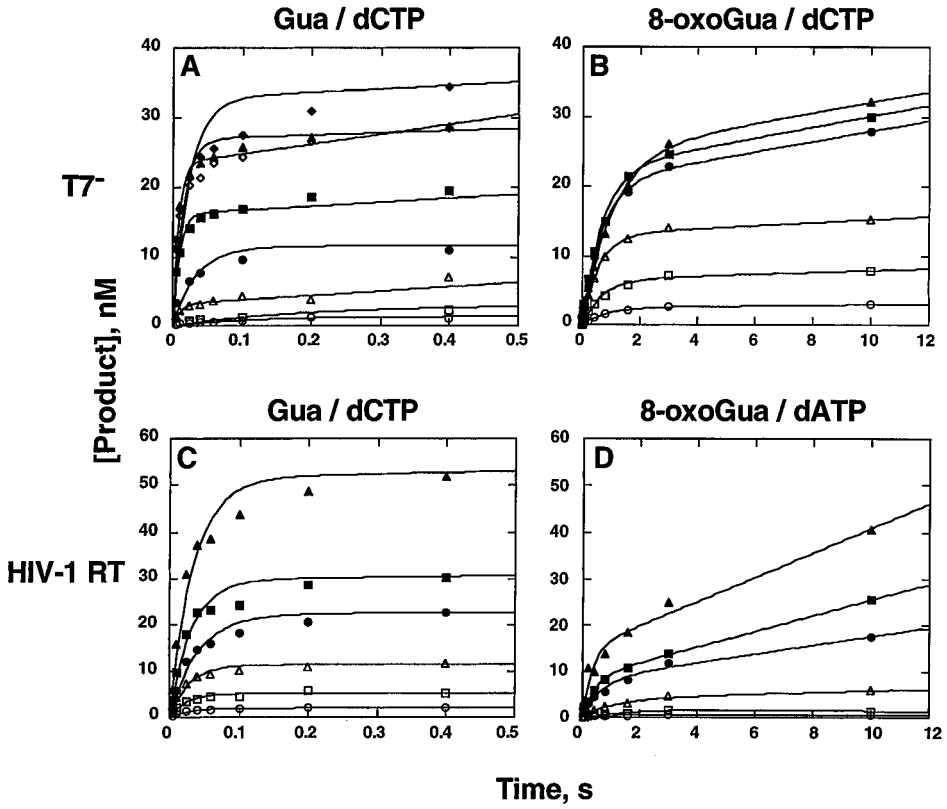

FIGURE 2: Active-site titration of enzyme−oligonucleotide complexes (E·DNA). (A) T7⁻ (28−33 nM) was preincubated with increasing concentrations of unmodified 24/36-mer (2 nM, ○; 5 nM, □ ; 12 nM, △; 23 nM, ●; 31 nM, ■; 47 nM, ▲; 83 nM, ◇; and 128 nM, ◆) and then mixed with a solution of dCTP (220 μM) in buffer A. The amplitude of the burst changed with the concentration of DNA. (B) T7⁻ (28−33 nM) was preincubated with increasing concentrations of 24-mer/8-oxoGua-modified 36-mer (5 nM, ○; 12 nM, □; 23 nM, △; 47 nM, ●; 82 nM, ■; 128 nM, ▲) and then mixed rapidly with a solution of dCTP (220 μM) in buffer A to start the reaction. The amplitude of the burst changed with the concentration of DNA. (C) HIV-1 RT [70−80 nM (32−36 nM active concentration)] was preincubated with increasing concentrations of unmodified 24/36-mer (4 nM, ○; 10 nM, □; 20 nM, △; 41 nM, ●; 82 nM, ■; 128 nM, ▲) and then mixed rapidly with a solution of dCTP (220 μM) in buffer A to start the reaction. (D) HIV-1 RT [70−80 nM (32−36 nM active concentration)] was preincubated with increasing concentrations of 24-mer/8-oxoGua-modified 36-mer (4 nM, ○; 10 nM, □; 20 nM, △; 41 nM, ●; 82 nM, ■; 128 nM, ▲) and then mixed rapidly with a solution of dATP (220 μM) in buffer A to start the reaction. The solid lines represent a fit of the data to the equation $y = A(1 - e^{-kpt}) + k_{ss}t$ as described in Experimental Procedures.

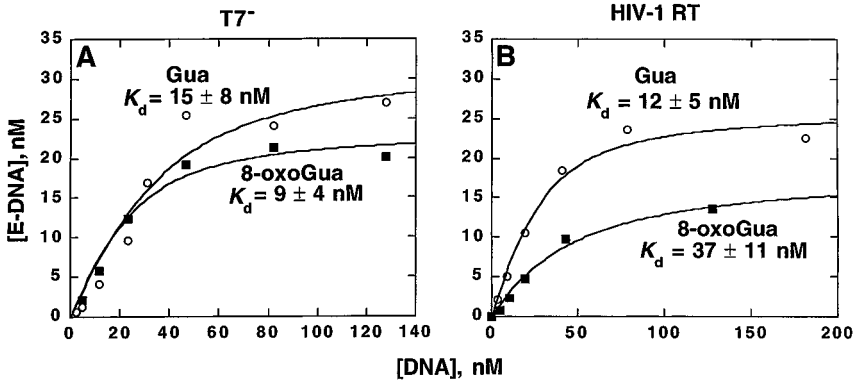

FIGURE 3: Determination of K_d^{DNA}. (A) The plots are of the burst amplitude for incorporation of dCTP by T7⁻ opposite Gua (○) or opposite 8-oxoGua (■) as determined from the experiments shown in Figure 2A,B versus the respective 24/36-mer concentrations. The solid lines are fits of the points to the quadratic equation $[E{\cdot}D] = 0.5(K_d + E_t + D_t) - [0.25(K_d + E_t + D_t)^2 - E_tD_t]^{1/2}$, where E_t = [total enzyme], D_t = [total DNA], and K_d = dissociation constant for the reaction E + D ⇌ E·D. The K_d values for T7⁻ binding unmodified (15 ± 8 nM) and 24-mer/8-oxoGua-modified 36-mer (9 ± 4 nM) are thought not to differ. (B) The plots are of the burst amplitude for incorporation of dCTP by HIV-1 opposite Gua (○) or of dATP opposite 8-oxoGua (■) as determined from the experiments shown in Figure 2C,D versus the respective 24/36-mer concentrations. The solid lines are fits of the points to the quadratic equation described above. The K_d values for HIV-1 RT binding of unmodified 24/36-mer (○) (12 ± 5 nM) and 24-mer/8-oxoGua-modified 36-mer (■) (37 ± 11 nM) are different.

the conformational change before chemistry and chemistry. This notation is necessary since we are unable (in rapid quench assays) to uncouple conformational change and chemistry (Patel et al., 1991). The k_p values for incorporation by T7⁻ of dCTP opposite either Gua or 8-oxoGua were found to be 80 ± 8 and 1.6 ± 0.1 s^{-1}, a difference of ∼50-fold, while K_d values differed by ∼3-fold (2.9 ± 1.4 μM for incorporation of dCTP opposite Gua and 11 ± 3 μM for incorporation of dCTP opposite 8-oxoGua) (Figure 5A,B). The k_p for incorporation of dATP opposite 8-oxoGua by T7⁻ was estimated to be ∼0.2 s^{-1} by dividing the slope of the time progress curve (Figure 1C) by the concentration of enzyme (Table 4). This value is greater than the steady-state determined k_{cat} value of ∼0.03 s^{-1}. The K_d for binding

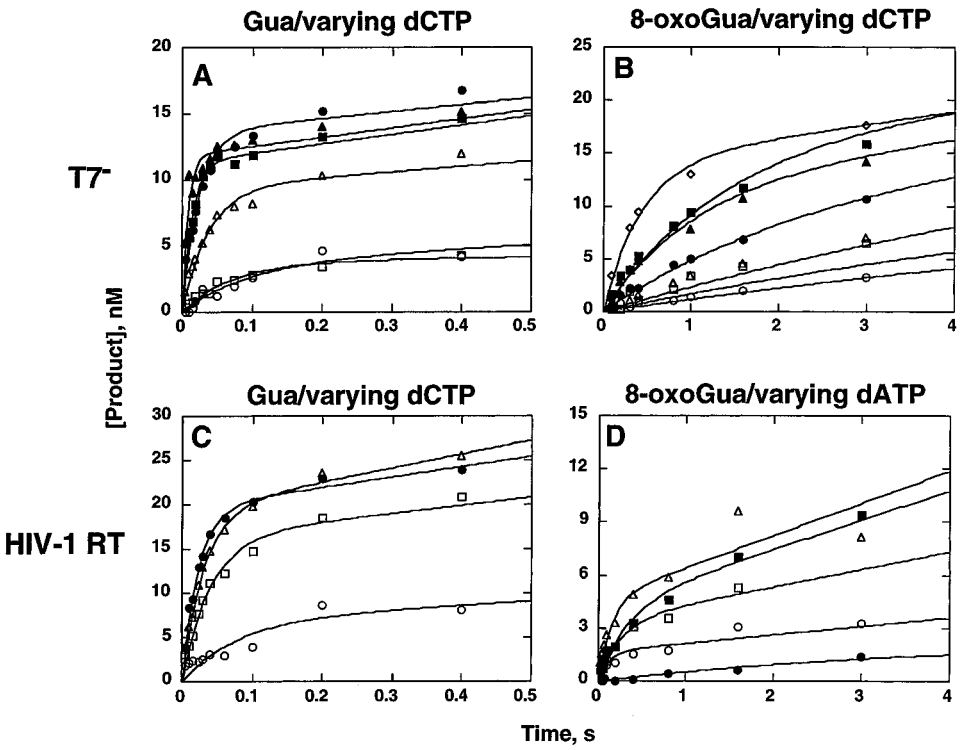

FIGURE 4: dNTP concentration dependence of the pre-steady-state burst rate. (A) A preincubated solution of T7$^-$ (25−30 nM) and unmodified 24/36-mer (102 nM) was mixed with increasing concentrations of dCTP (1.7 μM, ○; 5.5 μM, □; 11 μM, △; 22 μM, ●; 44 μM, ■; and 88 μM, ▲) in buffer A to start the reactions. The reactions were quenched over a time range of 0.005−3 s. (B) A preincubated solution of T7$^-$ (25−30 nM) and 8-oxoGua-modified 24/36-mer (102 nM) was mixed with increasing concentrations of dCTP (11 μM, ○; 44 μM, □; 72 μM, △; 88 μM, ●; 165 μM, ■; 220 μM, ▲; and 440 μM, ◇) in buffer A to start the reactions. The reactions were quenched over a time range of 0.1−20 s. (C) A preincubated solution of HIV-1 RT [70−80 nM (32−36 nM active concentration)] and unmodified 24/36-mer (102 nM) was mixed with increasing concentrations of dCTP (1.1 μM, ○; 11 μM, □; 22 μM, △; and 44 μM, ●) in buffer A to start the reactions. The reactions were quenched over a time range of 0.005−0.4 s. (D) A preincubated solution of HIV-1 RT [70−80 nM (32−36 nM active concentration)] and 8-oxoGua-modified 24/36-mer (102 nM) was mixed with increasing concentrations of dATP (1.1 μM, ●; 5.5 μM, ○; 28 μM, ■; 110 μM, □; and 220 μM, △) in buffer A to start the reactions. The reactions were quenched over a time range of 0.1−3 s. The solid lines represent a fit of the data to the equation $y = A(1 - e^{-k_p t}) + k_{ss}t$ as described in Experimental Procedures.

dATP was estimated by competition assays (*vide infra*).

The k_p for incorporation of dCTP opposite Gua by HIV-1 RT was determined to be 42 ± 5 s^{-1} by the method described above of varying dCTP and measuring changes in pre-steady-state rates (Figures 4C and 5C). Since there was no burst of product formation for incorporation of dCTP opposite 8-oxoGua, the k_p was estimated by dividing the slope of the time progress curve (Figure 1E) by the concentration of enzyme, yielding a k_p of ∼0.2 s^{-1}, a k_p value 200-fold lower than that for insertion of dATP opposite 8-oxoGua. The K_d for incorporation of dCTP opposite 8-oxoGua was determined by competition assays described later. The k_p and K_d for incorporation of dATP opposite 8-oxoGua by HIV-1 RT could be determined by measuring the changes in pre-steady-state rates as a function of [dATP] (Figure 4D). This analysis produced a k_p of 1.3 ± 0.2 s^{-1} and a K_d of 10 ± 6 μM for insertion of dATP opposite 8-oxoGua by HIV-1 RT (Figure 5D).

Competition Assays To Determine $K_{d,app}$ for Incorporation of dATP Opposite 8-OxoGua by T7$^-$ and $K_{d,app}$ for Incorporation of dCTP Opposite 8-OxoGua by HIV-1 RT. In order to estimate the apparent binding affinity of T7$^-$ for dATP and of HIV-1 RT for dCTP, competition assays were done. Assays with T7$^-$ contained 20 or 60 μM dCTP with a 125 μCi spike of [α-^{32}P]dCTP and either 0, 20, 60, or 200 μM unlabeled dATP. The 8-oxoGua-containing DNA substrate duplex was not labeled in these experiments. Reactions were initiated by the addition of dNTPs plus Mg^{2+}, as described for the other rapid quench assays. Time points were taken from 60 ms to 20 s. Bands corresponding to extension at 8-oxoGua by labeled dCTP were quantitated in the usual way except the band volume was converted directly into concentration of product by comparison of product formation at the same time points in experiments with labeled oligo and cold dCTP (Figure 6A and data not shown). As the concentration of competitor (dATP) was increased, the rate was decreased (Figure 6A and results not shown). The rate was decreased by 50% when the concentration of dATP was ∼10-fold greater than the concentration of dCTP. This result suggests that the $K_{d,app}^{dATP}$ is ∼110 μM.

Mixtures for competition reactions with HIV-1 RT contained 20 μM dATP with a 125 μCi spike of [α-^{32}P]dATP and either 0, 20, 60, or 200 μM unlabeled dCTP. Reactions were performed as described above for T7$^-$. As the concentration of competitor, dCTP in this case, was increased, the rate was decreased (Figure 6B). The rate was decreased by 50% when the concentration of dCTP was ∼10-fold greater than the concentration of dATP, predicting a $K_{d,app}^{dCTP}$ of ∼100 μM.

Next Correct Base Addition Following a C·8-OxoGua or an A·8-OxoGua Base Pair. Steady-state work with KF$^+$ and pol α and pre-steady-state studies with KF$^-$ and pol II$^-$ showed that extension past a C·8-oxoGua pair was slow while extension of an A·8-oxoGua pair occurs readily (Lowe & Guengerich, 1996; Shibutani et al., 1991). The current work with T7$^-$ and HIV-1 RT is consistent with those findings. The general approach for the extension experiments has been described (Lowe & Guengerich, 1996).

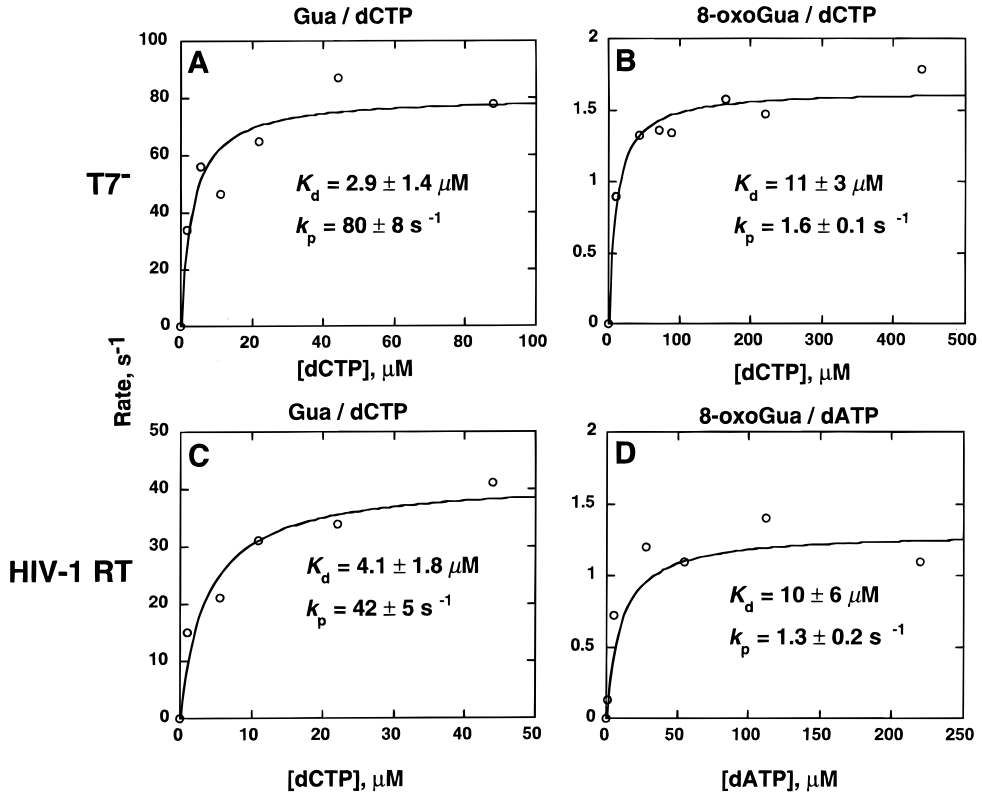

FIGURE 5: Determination of pre-steady-state K_d and k_p values. (A) A preincubated solution of T7⁻ (25−30 nM) and 102 nM unmodified 24/36-mer was mixed with increasing concentrations of dCTP (1.7−88 μM) in buffer A over a time range of 0.005−0.4 s, as shown in Figure 4A. The pre-steady-state rates of product formation were determined by single-exponential analysis of the burst phase (see the text for explanation) and then plotted against [dCTP] to determine K_d and k_p for incorporation of dCTP opposite Gua by T7⁻. (B) A preincubated solution of T7⁻ (25−30 nM) and 102 nM 8-oxoGua-modified 24/36-mer was mixed with increasing concentrations of dCTP (11−440 μM) in buffer A over a time range of 0.1−4 s, as shown in Figure 4B. The pre-steady-state rates of product formation were determined by single-exponential analysis of the burst phase (see the text for explanation) and then plotted against [dCTP] to determine K_d and k_p for incorporation of dCTP opposite 8-oxoGua by T7⁻. (C) A preincubated solution of HIV-1 RT [70−80 nM (32−36 nM active concentration)] and 102 nM unmodified 24/36-mer was mixed with increasing concentrations of dCTP (1.1−44 μM) in buffer A over a time range of 0.005−0.4 s, as shown in Figure 4C. The pre-steady-state rates of product formation were determined by single-exponential analysis of the burst phase (see the text for explanation) and then plotted against [dCTP] to determine K_d and k_p for incorporation of dCTP opposite Gua by HIV-1 RT. (D) A preincubated solution of HIV-1 RT [70−80 nM (32−36 nM active concentration)] and 102 nM 8-oxoGua-modified 24/36-mer was mixed with increasing concentrations of dATP (5.5−220 μM) in buffer A over a time range of 0.1−4 s, as shown in Figure 4D. The pre-steady-state rates of product formation were determined by single-exponential analysis of the burst phase (see the text for explanation) and then plotted against [dATP] to determine K_d and k_p for incorporation of dATP opposite 8-oxoGua by HIV-1 RT. The solid lines represent the fit of the rate data to the hyperbola $k_{obs} = [k_p[dNTP]/([dNTP] + K_d)]$.

Table 4: Pre-Steady-State Kinetic Parameters for dNTP Incorporation by T7⁻ and HIV-1 RT[a]

	T7⁻		HIV-1 RT	
	K_d (μM)	k_p (s^{-1})	K_d (μM)	k_p (s^{-1})
G·C[b]	2.9 ± 1.4	80 ± 8	4.1 ± 1.8	42 ± 5
8-oxoG·C[b]	11 ± 3	1.6 ± 0.1	∼100[c]	∼0.2[d]
8-oxoG·A[b]	∼110[c]	∼0.2[d]	10 ± 6	1.3 ± 0.2

[a] Values for k_{ss}, the "steady-state" rate of the multiple-turnover phase of the progress curves, were estimated by dividing the slopes of that portion of the curves by the concentration of enzyme. Values with T7⁻ and G·C and 8-oxoG·C were approximately 0.2 and 0.1 s^{-1}, respectively. The values with HIV-1 RT and G·C and 8-oxoG·A were approximately 0.1 and 0.1 s^{-1}, respectively. [b] The base in the oligomer is presented first (G or 8-oxoG), followed by the dNTP used (C or A). [c] Estimates based on competition assays containing dCTP and dATP. See Figure 6 and the text for discussion. [d] Estimates made by dividing the slope of the progress curves (Figure 1C, F) by the enzyme concentration.

Briefly, enzyme was preincubated with unmodified 36-mer annealed to a "25C" or "25A" primer so that a C·G or an A·G base pair was formed, respectively, or enzyme was preincubated with 8-oxoGua-modified 36-mer annealed to a 25C or 25A primer so that a C·8-oxoGua or an A·8-oxoGua base pair was formed, respectively (Scheme 2). Reactions were initiated by addition of the next correct nucleotide (dGTP, 220 μM) plus $MgCl_2$. Both T7⁻ and HIV-1 RT efficiently extended the G·C base pair with pre-steady-state rates of ∼116 and ∼43 s^{-1}, respectively (Figure 7A,C). The G·A base pair proved to be a block to both polymerases (Figure 7A,C). Extension of the 8-oxoGua·A base pair by T7⁻ occurred with a pre-steady-state rate of ∼80 s^{-1} (Figure 7B). Also, extension of the 8-oxoGua·C base pair by T7⁻ occurred but with a pre-steady-state rate of only ∼15 s^{-1}. HIV-1 RT extended the 8-oxoGua·A base pair with a pre-steady-state rate of ∼28 s^{-1}, ∼60% of the rate for incorporation after the G·C base pair (Figure 7D). The 8-oxoGua·C base pair was partially blocking to HIV-1 RT (Figure 7D).

DISCUSSION

Kinetic and fidelity differences among DNA polymerases that share similar structures and mechanisms of action have been described in many systems in the literature. Since the fidelity of individual polymerases contributes to the overall fidelity of DNA replication, understanding the differences in the kinetics of stepwise polymerization by various polymerases will increase the understanding of how DNA adducts are misreplicated and correctly replicated and of how

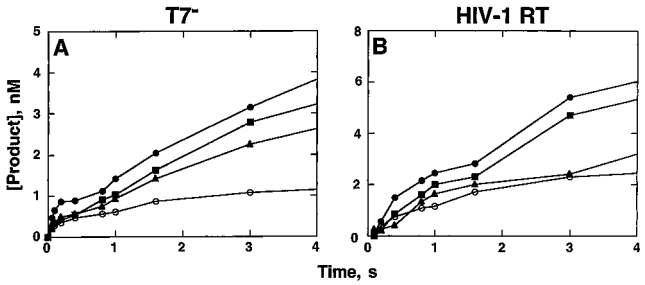

FIGURE 6: Competition assays to estimate $K_{d,app}$. (A) Estimation of $K_{d,app}$ for T7$^-$ binding of dATP in the presence of 8-oxoGua-modified 24/36-mer substrate. Assays were carried out with T7$^-$ (27−36 nM), 102 nM 8-oxoGua-modified 24/35-mer (not radiolabeled), 20 μM dCTP plus a 125 μCi spike of [α-^{32}P]dCTP, and various concentrations of dATP. Reaction sets were 20 μM dCTP/0 μM dATP (●); 20 μM dCTP/20 μM dATP (■), 20 μM dCTP/60 μM dATP (▲), and 20 μM dCTP/200 μM dATP (○). Primer extension was measured by incorporation of radiolabeled dCTP. As the concentration of cold dATP was increased, the signal produced by incorporation of radiolabeled dCTP was decreased. With the conversion of band volumes determined from the Imagequant software to [product], the $K_{d,app}{}^{dATP}$ was estimated to be ~10-fold greater than the $K_d{}^{dCTP}$. (B) Estimation of $K_{d,app}$ for HIV-1 RT binding of dCTP in the presence of 8-oxoGua-modified 24/36-mer substrate. Assays were carried out with HIV-1 RT [100 nM (45 nM active concentration)], 102 nM 8-oxoGua-modified 24/35-mer (not radiolabeled), 20 μM dATP plus a 125 μCi spike of [α-^{32}P]dATP, and various concentrations of dCTP. Reaction sets were 20 μM dATP/0 μM dCTP (●); 20 μM dATP/20 μM dCTP (■), 20 μM dATP/60 μM dCTP (▲), and 20 μM dATP/200 μM dCTP, (○). Primer extension was measured by incorporation of radiolabeled dATP. As the concentration of cold dCTP was increased, the signal produced by incorporation of radiolabeled dATP was decreased. As in part A, the $K_{d,app}{}^{dCTP}$ was estimated to be ~10-fold greater than the $K_d{}^{dATP}$.

Scheme 2: Extension of A·8-OxoGua and C·8-OxoGua Base Pairs

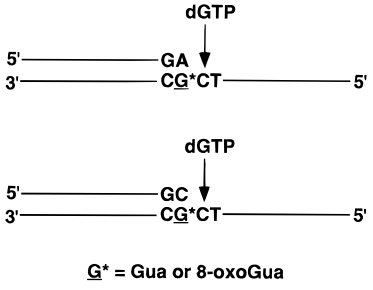

the mutagenic potential of an adduct will change depending on the polymerase responsible for the replication event. In the present study, the pre-steady-state kinetics of replication of 8-oxoGua by the viral replicative enzymes T7$^-$ and HIV-1 RT were analyzed in order to determine how nucleotide incorporation at and beyond 8-oxoGua by replicative enzymes varies with that by *E. coli* repair enzymes.

The steady-state K_m values for insertion of dCTP and dATP opposite 8-oxoGua by T7$^-$ were 22- and 55-fold greater, respectively, than the K_m for insertion of dCTP opposite Gua (Table 2). However, k_{cat} values for insertion of dCTP or dATP opposite 8-oxoGua-modified T7$^-$ were only ~5-fold lower than the k_{cat} value for dCTP addition opposite Gua. Steady-state analysis was also performed with HIV-1 RT. The differences between K_m for insertion of dCTP and dATP opposite 8-oxoGua and K_m for insertion of dCTP opposite Gua were ~200 and ~100 greater, respectively, while there was little difference in k_{cat} values for incorporation of dATP opposite 8-oxoGua and of dCTP opposite Gua. Insertion of dCTP opposite 8-oxoGua by HIV-1 RT did show a 5-fold lower k_{cat}. From steady-state analysis of this type, it would appear that polymerase discrimination for insertion of the correct base versus the incorrect base occurs at the level of K_m, though the exact meaning of K_m in these experiments is not well defined (Johnson, 1992, 1993, 1995). Pre-steady-state, single-turnover kinetics were used in an endeavor to understand more fully the kinetic contributions to misincorporation opposite 8-oxoGua.

Pre-steady-state kinetics allow for the distinction of single turnovers from multiple turnovers when a biphasic response is observed [for review, see Johnson (1995)]. In this case, a rate-limiting step within the burst phase and for the overall mechanism (i.e., multiple turnovers, steady state) can be described. Also, the steady-state rate-limiting step must occur after chemistry. The rate-limiting step in the burst phase (first cycle) would be a step at or before chemistry. If chemistry is the rate-limiting step within the burst phase (first reaction cycle), use of the thio analog for the normal dNTP should extinguish the burst of product formation by at least 10-fold (Herschlag et al., 1991). If there is no thio effect, a step before chemistry is assumed to be rate-limiting in the first reaction cycle. In the absence of a biphasic response, chemistry or a step before chemistry is assumed to be rate-limiting in the steady state. If chemistry is the rate-limiting step, use of the thio analog should reduce the rate of product formation.

The first set of pre-steady-state experiments was time progress curves with which the kinetics of the reactions were examined, i.e., biphasic or not biphasic (Figure 1). Incorporation of dCTP opposite Gua by T7$^-$ and HIV-1 RT showed a burst of product formation followed by a slower multiple-turnover rate. This result suggests that a step after chemistry is rate-limiting in the steady state with these polymerases in the normal incorporation reaction, as noted with KF$^-$ and pol II$^-$ (Mizrahi et al., 1985; Lowe & Guengerich, 1996). Incorporation of dCTP opposite 8-oxoGua by T7$^-$ also shows a burst of product formation, again suggesting a steady-state rate-limiting step after chemistry. Insertion of dATP opposite 8-oxoGua by T7$^-$ does not show a burst of product formation, indicating that chemistry or a step before chemistry is rate-limiting in the steady state. These findings are similar to those reported for the kinetics of KF$^-$ and pol II$^-$ (Lowe & Guengerich, 1996). In the case of HIV-1 RT, the situation is somewhat different. HIV-1 RT shows a burst of product formation for insertion of dATP opposite 8-oxoGua but not for insertion of dCTP opposite 8-oxoGua. With HIV-1 RT, unlike the other polymerases, chemistry does not appear to be the steady-state rate-limiting step during addition of dATP opposite 8-oxoGua.

These findings were explored further in phosphorothioate substitution reactions. In this case, the normal dNTPs were substituted with their corresponding phosphorothioate analogs. Substitution of sulfur for phosphate at the α-position of the triphosphate will decrease the chemical reactivity of the dNTP (Benkovic & Schray, 1973). If chemistry is a mechanism rate-limiting step, use of the analog should reduce or extinguish the burst of product formation. When dCTPαS was used with T7$^-$ and HIV-1 RT for incorporation opposite Gua, there was no difference in the burst curve, suggesting that chemistry is not a rate-limiting step in the mechanism (Figure 1A,D). Substitution of thio analogs for incorporation opposite 8-oxoGua by T7$^-$ eliminated the burst of product formation seen with dCTP and further eliminated the amount

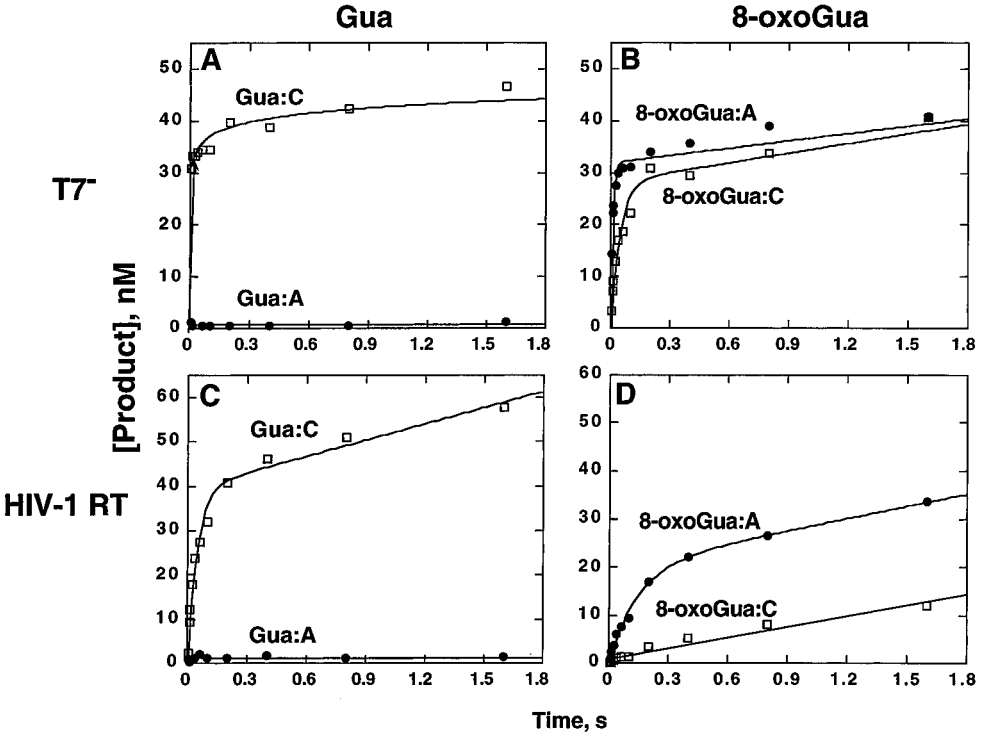

FIGURE 7: Extension past C·G, C·8-oxoGua, A·G, and A·8-oxoGua base pairs. (A) T7⁻ (30 nM) was preincubated with unmodified template annealed to either a 25C (□) or 25A (●) primer (102 nM) so that a C·G or an A·G base pair was formed, respectively (see Scheme 2). Extension reactions were initiated by the addition of 220 μM dGTP in buffer A. (B) T7⁻ (30 nM) was preincubated with 8-oxoGua-modified template annealed to either a 25C (□) or 25A (●) primer (102 nM) so that a C·8-oxoGua or an A·8-oxoGua base pair was formed, respectively. Extension reactions were initiated by the addition of 220 μM dGTP in buffer A. (C) HIV-1 RT [89 nM (40 nM active concentration)] was preincubated with unmodified template annealed to either a 25C (□) or 25A (●) primer (102 nM) so that a C·G or an A·G base pair was formed, respectively. Extension reactions were initiated by the addition of 220 μM dGTP in buffer A. (D). HIV-1 RT [89 nM (40 nM active concentration)] was preincubated with 8-oxoGua-modified template annealed to either a 25C (□) or 25A (●) primer (102 nM) so that a C·8-oxoGua or an A·8-oxoGua base pair was formed, respectively. Extension reactions were initiated by the addition of 220 μM dGTP in buffer A.

of product formed during incorporation of dATP opposite 8-oxoGua. This result is consistent with the pattern of thio effects noted with KF⁻ and pol II⁻ (Lowe & Guengerich, 1996). When thio analogs were used for incorporation opposite 8-oxoGua by HIV-1 RT, only a modest thio effect for incorporation of dATP was observed (~2) and the amount of product formed by addition of dCTP was not significantly decreased, though the slow rate of the reaction with dCTP makes accurate determination of a thio effect difficult and the data do not allow a clear assessment of whether chemistry is rate-limiting during incorporation of dCTP opposite 8-oxoGua by HIV-1 RT. This result diverges from what has been noted for KF⁻, pol II⁻, and T7⁻ in that it suggests that chemistry is not a mechanism rate-limiting step for incorporation of dATP and possibly of dCTP opposite 8-oxoGua by HIV-1 RT. Thio analyses of normal misincorporation reactions (i.e., in the absence of DNA adducts) with HIV-1 RT have not been reported in the literature to our knowledge, although thio substitution reactions during correct incorporations by HIV-1 RT have shown no thio effect (Hsieh et al., 1993; Kati et al., 1992). Zinnen et al. (1994) have shown thio effects for incorporation of a correct base following a mispair. Thus, the chemistry of HIV-1 RT can be rate-limiting under certain conditions, but the presence of 8-oxoGua does not cause chemistry to be rate-limiting.

Previous work with KF⁻ and pol II⁻ showed no discrimination in binding unmodified and 8-oxoGua-modified DNA substrates, and the K_d^{DNA} values for the polymerases were similar (~10 nM for KF⁻ and ~20 nM for pol II⁻) (Lowe & Guengerich, 1996). Other studies that have examined the ability of various DNA polymerases to bind a variety of substrates, including those with mismatched termini and blunt ends, have shown that the DNA polymerases are capable of efficiently binding these substrates (Zinnen et al., 1994; Kuchta et al., 1988; Creighton et al., 1992; Yu & Goodman, 1992; Mendelman et al., 1990). The K_d values determined for T7⁻ with unmodified and 8-oxoGua-modified templates were similar to those found with KF⁻ and pol II⁻ (~10 nM). The K_d value determined for HIV-1 RT and unmodified substrate is also similar to those for KF⁻, pol II⁻, and T7⁻ (~12 nM), but the K_d value for HIV-1 RT and 8-oxoGua-modified substrate is slightly higher (37 ± 11 nM). This difference may be due to the presence of enzyme−DNA complexes that are not competent for dNTP insertion. The maximum amplitude for the burst for insertion of dATP opposite 8-oxoGua by HIV-1 RT is later than the maximum for insertion of dCTP opposite Gua (1600 versus 200 ms). The reduced single-turnover rate and slightly reduced amplitude may be attributed to the formation of nonproductive complexes of HIV-1 RT and 8-oxoGua-modified substrate. Precedence for this explanation comes from several laboratories (Zinnen et al., 1994; Latham & Lloyd, 1994; Kati et al., 1992). Zinnen et al. (1994) noted a less than full burst amplitude for HIV-1 RT correct incorporation following a mispair. Following analysis of the possible explanations for the reduced burst, they attributed the reduced burst to the existence of an HIV-1 RT·DNA complex in two states, only one of which is capable of efficient extension. Kati et al. (1992) suggested that HIV-1 RT·DNA·dNTP complexes can exist in alternate conformations with differing

stabilities. That is, an "off-pathway" conformational change prior to chemistry may sequester pools of E·D·N in an "inactive" state. Furthermore, Kati et al. (1992) suggest that the rate of isomerization between the two conformational states can be reduced in the presence of mismatches in the new base pair. On the basis of kinetic simulations of our data (Table 3), the conformation change before chemistry appears to be the mechanism rate-limiting step for addition of dATP and dCTP opposite 8-oxoGua, and this may facilitate the formation of inactive complexes which would yield a reduced burst amplitude. The basis of this phenomenon should become more apparent from a physical study of the interaction of HIV-1 RT with the 8-oxoGua-modified substrate. Overall, the K_d^{DNA} values of the four polymerases with the unmodified and 8-oxoGua-modified substrates do not differ greatly, consistent with what is known about polymerase binding of various DNA substrates [for review see Johnson 1993)].

The dependence of the burst rate on dNTP concentration was determined, including the pre-steady-state parameters K_d and k_p (Figures 4 and 5). Experiments with T7$^-$ showed the K_d^{dCTP} with 8-oxoGua-modified template to be ~4-fold greater than that with unmodified template. Furthermore, from competition assays, the $K_{d,app}^{dATP}$ was estimated to be ~10-fold greater than the K_d^{dCTP} in reactions with 8-oxoGua-containing template (Figure 6A). The k_p for insertion of dCTP (1.6 ± 0.1 s^{-1}) was also around 10-fold greater than the k_p for insertion of dATP (0.2 s^{-1}) opposite 8-oxoGua. Experiments with KF$^-$ and pol II$^-$ showed ~20-fold differences in k_p values for incorporation of dCTP versus dATP opposite 8-oxoGua. The k_p for insertion of dCTP opposite Gua by T7$^-$ was 50-fold greater than that for insertion of dCTP opposite 8-oxoGua (80 ± 8 s^{-1} versus 1.6 ± 0.1 s^{-1}). HIV-1 RT showed the smallest differences among the four polymerases in k_p values for insertion of dCTP versus dATP opposite 8-oxoGua. Incorporation of dATP opposite 8-oxoGua occurred at a rate that was ~7-fold faster than that for incorporation of dCTP opposite 8-oxoGua (1.3 ± 0.2 versus 0.2 s^{-1}), while the normal incorporation reaction (dCTP opposite Gua) occurred at a rate that was ~200-fold faster than that for incorporation of dCTP opposite 8-oxoGua (42 ± 5 s^{-1} versus 0.2 s^{-1}). From competition assays, the $K_{d,app}^{dCTP}$ was found to be ~10-fold greater than K_d^{dATP}.

Kinetic simulations of observed kinetic curves provide useful information in terms of approximating rate constants for a defined mechanistic pathway. Using the dNTP dependence curves (Figure 4 and data not shown), a set of parameters consistent with the proposed mechanism in Scheme 1 of T7$^-$ and HIV-1 RT were determined (Table 3). This type of analysis has been used to provide quantitative estimates of the rate constants governing the mechanism of polymerization by KF$^+$, KF$^-$, T7 DNA polymerase, HIV-1 RT, and pol II$^-$ (Eger & Benkovic, 1992; Kuchta et al., 1988; Wong et al., 1991; Donlin et al., 1991; Kati et al., 1992; Lowe & Guengerich, 1996). From the kinetic simulations, the largest differences between incorporation of dCTP and dATP opposite 8-oxoGua were noted in steps 3 and 4, i.e., conformational change prior to chemistry (k_3) and chemistry (k_4) (Table 3). These same steps were the most affected in simulations done previously with KF$^-$ and pol II$^-$, though the magnitudes of the differences between the steps are different. From simulations with KF$^-$ and pol II$^-$, chemistry (k_4) appears to be the rate-limiting step, while the present simulations with T7$^-$ and HIV-1 RT show that the mechanism rate-limiting step receives contributions from both chemistry (k_4) and the conformational change before chemistry (k_3). Previous work with unmodified DNA has suggested that T7$^-$ and HIV-1 RT show larger discrimination in binding incorrect nucleotides than KF$^-$ (Friedberg et al., 1995). This would seem to be in contradiction to the simulation data shown here for T7$^-$ and HIV-1 RT and previous data for KF$^-$ (Lowe & Guengerich, 1996) since the simulations here do not show apparent differences in k_2 for incorporation of dCTP and dATP opposite 8-oxoGua as seen with KF$^-$ and pol II$^-$. However, contributions from the conformational change to dNTP discrimination are much greater here than with KF$^-$, suggesting that the discrimination may be more a result of slowed conformational change than initial substrate selection in the presence of 8-oxoGua. These discrepancies would be better understood by the experimental decoupling of the chemistry and conformational change steps. Kinetic simulations comparing incorporation of dCTP and dATP opposite 8-oxoGua by T7$^-$ showed a 7-fold difference in the rates of the conformational change prior to chemistry while chemistry rates (k_4) varied by ~2−5-fold. Rate constants simulated for HIV-1 RT incorporation of dCTP and dATP opposite 8-oxoGua showed a 100-fold difference in the rate of the conformational change prior to chemistry and at least a 10-fold difference in the rate of chemistry, with the rates for incorporation of dATP being greater than those for insertion of dCTP. The results of the simulations of HIV-1 RT incorporation of dATP opposite 8-oxoGua are consistent with the experimental data in that chemistry does not appear to be rate-limiting while the conformational change rate does appear to be rate-limiting. This supports the theory that pools of HIV-1 RT·DNA·dNTP are sequestered in an inactive state, thus yielding reduced burst rates and amplitudes (*vide supra*). Simulations from studies with KF$^-$ and pol II$^-$ showed that, when dCTP or dATP is incorporated opposite 8-oxoGua, k_4 becomes at least partially rate-limiting (Lowe & Guengerich, 1996).

Incorporation of the next correct base following a mismatch normally occurs at a greatly reduced rate compared to incorporation following a Watson−Crick base pair (Echols & Goodman, 1991). The reduced rate appears to be attributable to a kinetic barrier to extension rather than to polymerase difficulty in binding mismatched termini (Echols & Goodman, 1991). In the present study, the ability of T7$^-$ and HIV-1 RT to extend 8-oxoGua·A and 8-oxoGua·C base pairs was examined (Figure 7 and Scheme 2). Both polymerases show more efficient extension of the 8-oxoGua·A base pair, consistent with previous findings for KF$^+$, KF$^-$, polymerase α, and pol II$^-$ (Lowe & Guengerich, 1996; Shibutani et al., 1991). The rate for addition of dGTP by T7$^-$ following the 8-oxoGua·A base pair is ~5-fold greater than the rate for addition of dGTP following the 8-oxoGua·C base pair (~80 s^{-1} versus ~15 s^{-1}). Likewise, HIV-1 RT prefers to extend the 8-oxoGua·A base pair, but at a rate that is ~60% of the rate for extension of a G·C base pair. The two mutagenic preferences of HIV-1 RT for inserting dATP opposite 8-oxoGua and for extending the 8-oxoGua·A base pair may be factors contributing to the lowered fidelity of HIV-1 RT compared to that of other polymerases which, though they extend the 8-oxoGua·A base pair more efficiently than an 8-oxoGua·C base pair, still prefer to insert dCTP opposite 8-oxoGua.

Analyses of the pre-steady-state kinetics of misincorporation opposite 8-oxoGua by repair and replicative poly-

merases reveal that the mutagenic potential of the adduct depends on mechanistic contributions from the enzyme's apparent K_d in binding correct and incorrect dNTPs, the ease of lesion extension, and either the rate of conformational change before chemistry or the rate of bond formation. Physical studies of the interactions of these enzymes with the adducted substrate and dNTP should provide further insight into the fidelity of nucleotide incorporation at the adduct.

ACKNOWLEDGMENT

We thank Dr. Carl Frieden for supplying the KINSIM program.

SUPPORTING INFORMATION AVAILABLE

Capillary gel electrophoretograms (2 pages). Ordering information is given on any current masthead page.

REFERENCES

Ames, B. N., Shigenaga, M. K., & Gold, L. S. (1993) *Environ. Health Perspect. 101* (Suppl. 5), 35−44.
Barshop, B. A., Wrenn, R. F., & Frieden, C. (1983) *Anal. Biochem. 130*, 134−145.
Basu, A. K., & Essigmann, J. M. (1988) *Chem. Res. Toxicol. 1*, 1−18.
Basu, A. K., & Essigmann, J. M. (1990) *Mutat. Res. 233*, 189−201.
Benkovic, S. J., & Schray, K. J. (1973) in *The Enzymes* (Boyer, P. D., Ed.) 3rd ed., Vol. 8, pp 201−236, Academic Press, New York.
Boosalis, M. S., Petruska, J., & Goodman, M. F. (1987) *J. Biol. Chem. 262*, 14689−14696.
Boosalis, M. S., Mosbaugh, D. W., Hamatake, R., Sugino, A., Kunkel, T. A., & Goodman, M. F. (1989) *J. Biol. Chem. 264*, 11360−11366.
Borer, P. N. (1975) in *Handbook of Biochemistry and Molecular Biology* (Fasman, G. D., Ed.) 3rd ed., pp 589−590, CRC Press, Cleveland, OH.
Cai, H., Bloom, L. B., Eritja, R., & Goodman, M. F. (1993) *J. Biol. Chem. 268*, 23567−23572.
Creighton, S., Huang, M.-M., Cai, H., Arnheim, N., & Goodman, M. F. (1992) *J. Biol. Chem. 267*, 2633−2639.
Donlin, M. J., Patel, S. S., & Johnson, K. A. (1991) *Biochemistry 30*, 538−546.
Echols, H., & Goodman, M. F. (1991) *Annu. Rev. Biochem. 60*, 477−511.
Eger, B. T., & Benkovic, S. J. (1992) *Biochemistry 31*, 9227−9236.
Feig, D. I., & Loeb, L. A. (1994) *J. Mol. Biol. 235*, 33−41.
Frey, M. W., Sowers, L. C., Millar, D. P., & Benkovic, S. J. (1995) *Biochemistry 34*, 9185−9192.
Friedberg, E. C., Walker, G. C., & Siede, W. (1995) in *DNA Repair and Mutagenesis*, pp 79−80, American Society for Microbiology Press, Washington, DC.
Herschlag, D., Piccirilli, J. A., & Cech, T. R. (1991) *Biochemistry 30*, 4844−4854.
Hsieh, J.-C., Zinnen, S., & Modrich, P. (1993) *J. Biol. Chem. 268*, 24607−24613.
Johnson, K. A. (1992) in *The Enzymes* (Boyer, P. D., Ed.) pp 1−61, Academic Press, New York.
Johnson, K. A. (1993) *Annu. Rev. Biochem. 62*, 685−713.
Johnson, K. A. (1995) *Methods Enzymol. 249*, 38−61.
Kati, W. M., Johnson, K. A., Jerva, L. F., & Anderson, K. S. (1992) *J. Biol. Chem. 267*, 25988−25997.
Kornberg, A., & Baker, T. A. (1992) in *DNA Replication*, pp 190, 221−222, W. H. Freeman, New York.
Kouchakdjian, M., Bodepudi, V., Shibutani, S., Eisenberg, M., Johnson, F., Grollman, A. P., & Patel, D. J. (1991) *Biochemistry 30*, 1403−1412.
Kuchta, R. D., Benkovic, P., & Benkovic, S. J. (1988) *Biochemistry 27*, 6716−6725.
Laemmli, U. K. (1970) *Nature 227*, 680−685.
Latham, G. J., & Lloyd, R. S. (1994) *J. Biol. Chem. 269*, 28527−28530.
Le Grice, S. F. J., & Grüninger-Leitch, F. (1990) *Eur. J. Biochem. 187*, 307−314.
Lipscomb, L. A., Peek, M. E., Morningstar, M. L., Verghis, S. M., Miller, E. M., Rich, A., Essigmann, J. M., & Williams, L. D. (1995) *Proc. Natl. Acad. Sci. U.S.A. 92*, 719−723.
Lowe, L. G., & Guengerich, F. P. (1996) *Biochemistry 35*, 9840−9849.
Lunn, C. A., Kathju, S., Wallace, B. J., Kushner, S. R., & Pigiet, V. (1984) *J. Biol. Chem. 259*, 10469−10474.
Malins, D. C., Polissar, N. L., Nishikida, K., Homes, E. H., Gardner, H. S., & Gunselman, S. J. (1995) *Cancer 75*, 503−517.
Marnett, L. J., & Burcham, P. C. (1993) *Chem. Res. Toxicol. 6*, 771−785.
McAuley-Hecht, K. E., Leonard, G. A., Gibson, N. J., Thomson, J. B., Watson, W. P., Hunter, W. N., & Brown, T. (1994) *Biochemistry 33*, 10266−10270.
Mendelman, L. V., Petruska, J., & Goodman, M. F. (1990) *J. Biol. Chem. 265*, 2338−2346.
Miller, E. C., & Miller, J. A. (1966) *Pharmacol. Rev. 18*, 805−838.
Miller, J. A., & Miller, E. C. (1971) *J. Natl. Cancer Inst. 47*, 5−14.
Mizrahi, V., Henrie, R. N., Marlier, J. F., Johnson, K. A., & Benkovic, S. J. (1985) *Biochemistry 24*, 4010−4018.
Patel, P. H., Jacobo-Molina, A., Ding, J., Tantillo, C., Clark, A. D., Jr., Raag, R., Nanni, R. G., Hughes, S. H., & Arnold, E. (1995) *Biochemistry 34*, 5351−5363.
Patel, S. S., Wong, I., & Johnson, K. A. (1991) *Biochemistry 30*, 511−525.
Perler, F. B., Kumar, S., & Kong, H. (1996) *Adv. Protein Chem. 48*, 377−435.
Reha-Krantz, L. J., Nonay, R. L., Day, R. S., & Wilson, S. H. (1996) *J. Biol. Chem. 271*, 20088−20095.
Shibutani, S., Takeshita, M., & Grollman, A. P. (1991) *Nature 349*, 431−434.
Shigenaga, M. K., Hagen, T. M., & Ames, B. N. (1994) *Proc. Natl. Acad. Sci. U.S.A. 91*, 10771−10778.
Shimoda, R., Nagashima, M., Sakamoto, M., Yamaguchi, N., Hirohashi, S., Yokota, J., & Kasai, H. (1994) *Cancer Res. 54*, 3171−3172.
Spence, R. A., Kati, W. M., Anderson, K. S., & Johnson, K. A. (1995) *Science 267*, 988−993.
Wong, I., Patel, S. S., & Johnson, K. A. (1991) *Biochemistry 30*, 526−537.
Yu, H., & Goodman, M. F. (1992) *J. Biol. Chem. 267*, 10888−10896.
Zinnen, S., Hsieh, J., & Modrich, P. (1994) *J. Biol. Chem. 269*, 24195−24202.

BI9627267